Remove the Residual Additives toward Enhanced Efficiency with Higher Reproducibility in Polymer Solar Cells

ARTICLE *in* THE JOURNAL OF PHYSICAL CHEMISTRY C · JULY 2013

Impact Factor: 4.77 · DOI: 10.1021/jp404395q

8 AUTHORS, INCLUDING:

Long Ye
North Carolina State University
52 PUBLICATIONS **1,457** CITATIONS
SEE PROFILE

Xia Guo
Soochow University (PRC)
72 PUBLICATIONS **3,628** CITATIONS
SEE PROFILE

Maojie Zhang
Soochow University (PRC)
65 PUBLICATIONS **2,443** CITATIONS
SEE PROFILE

Lijun Huo
Beihang University(BUAA)
56 PUBLICATIONS **3,943** CITATIONS
SEE PROFILE

THE JOURNAL OF PHYSICAL CHEMISTRY C

Article

pubs.acs.org/JPCC

Remove the Residual Additives toward Enhanced Efficiency with Higher Reproducibility in Polymer Solar Cells

Long Ye,[†,§,∥] Yan Jing,[†,∥] Xia Guo,[†,§] Hao Sun,[‡] Shaoqing Zhang,[†] Maojie Zhang,[†] Lijun Huo,[†] and Jianhui Hou*[,†]

[†]State Key Laboratory of Polymer Physics and Chemistry, Beijing National Laboratory for Molecular Sciences Institute of Chemistry, Chinese Academy of Sciences, Beijing 100190, China

[‡]Bruker Nano Surfaces Division, Bruker (Beijing) Scientific Technology Co. Ltd., Beijing 100081, China

[§]Graduate University of Chinese Academy of Sciences, Beijing 100049, China

Supporting Information

ABSTRACT: Undesirable efficiency reproducibility was sometimes observed in fabrication of high performance polymer solar cell devices incorporating high boiling point additives. The anomalous results originated from the slow drying of additives not only reduced the controllability of device performance but also impeded the studies of device physics and material design. How to remove the residual additives and achieve stable interface properties is crucial for both the academic and industrial community. Herein, we demonstrated that the morphological stability is enhanced and efficiency reproducibility is increased obviously from 7.07 ± 0.27% to 7.53 ± 0.12% after spin-coating inert solvents for the PBDTTT-C-T/PCBM system. The relationship between processing conditions and photovoltaic performance was well explored and demonstrated via multiple techniques including atomic force microscopy, Kelvin probe force microscopy, transmission electron microscopy, and X-ray photospectroscopy. Most importantly, this method was successfully employed in more than five representative donor polymers. Our study suggested that the slow drying process of the residual high boiling point additives could induce undesirable morphological variation as well as unfavorable interfacial contact, and by washing with low boiling point "inert" solvent, like methanol, the negative influence caused by the residual additive can be avoided and hence the additives would perform more efficiently in the optimization of device performance of highly efficient PSCs.

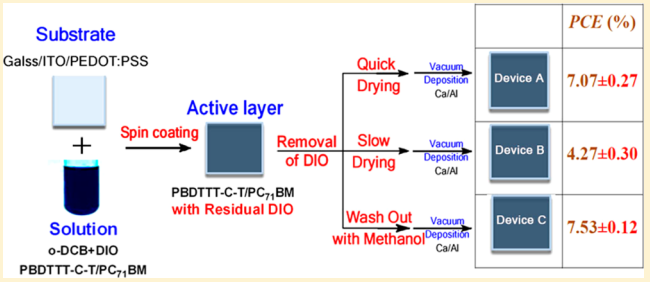

INTRODUCTION

Since the pioneering work of introducing 1,8-octanedithiol (OT) as solvent additive in fabrication process of bulk-heterojunction (BHJ) polymer solar cells (PSCs),[1] various high boiling point (T_B) solvent additives including 1,8-diiodooctane (DIO),[2] 1-chloronaphthalene (CN),[3,4] *N*-methyl-2-pyrrolidone (NMP),[3,5] nitrobenzene (NtB),[6] etc., have been employed in PSC device fabrication, which contributes greatly to the improvement of photovoltaic performance of PSCs as well as the understanding of morphology modulation. Among these, DIO has proved to be the most successful additive in device fabrications of highly efficient PSCs based on different polymer and [6, 6]-phenyl-C_{71}-butyric acid methyl ester ($PC_{71}BM$) blends.[7−19]

In our recent works, DIO also played an important role in exploring photovoltaic performance of novel polymers.[7−11,18−21] However, when DIO was used as additive, sometimes we found that poor reproducibility, i.e., great batch-to-batch variation of device performance, can be observed. In the worst case, S-shape *J*−*V* curves (S-curves for short), as shown in Figure 1a, were recorded sometimes, and meanwhile the key parameters, short-circuit current density (J_{sc}), open-circuit voltage (V_{oc}), and fill factor (FF), obtained from the S-curves are obviously lower than those from the normal curve. This kind of undesirable results not only reduced the reproducibility of device performance but also impeded the studies of device physics and material design; i.e., sometimes the batch-to-batch variation is so big that eventually it may conceal the real results. Therefore, to identify the origin of the S-curves and explore a feasible method to solve the problem will be of great importance to both the fundamental study and the industrial application of PSCs.

In view of the low saturated vapor pressure (~1×10^{-2} Pa) of DIO at room temperature (for details see the Supporting Information), DIO shows extremely low drying speed under ambient temperature and pressure. Actually, we observed that when 3−5% DIO was used as additive, the blend films obtained from spin-coating cannot be fully dried under ambient

Received: February 22, 2013
Revised: June 23, 2013
Published: July 11, 2013

   dx.doi.org/10.1021/jp404395q | *J. Phys. Chem. C* 2013, 117, 14920−14928

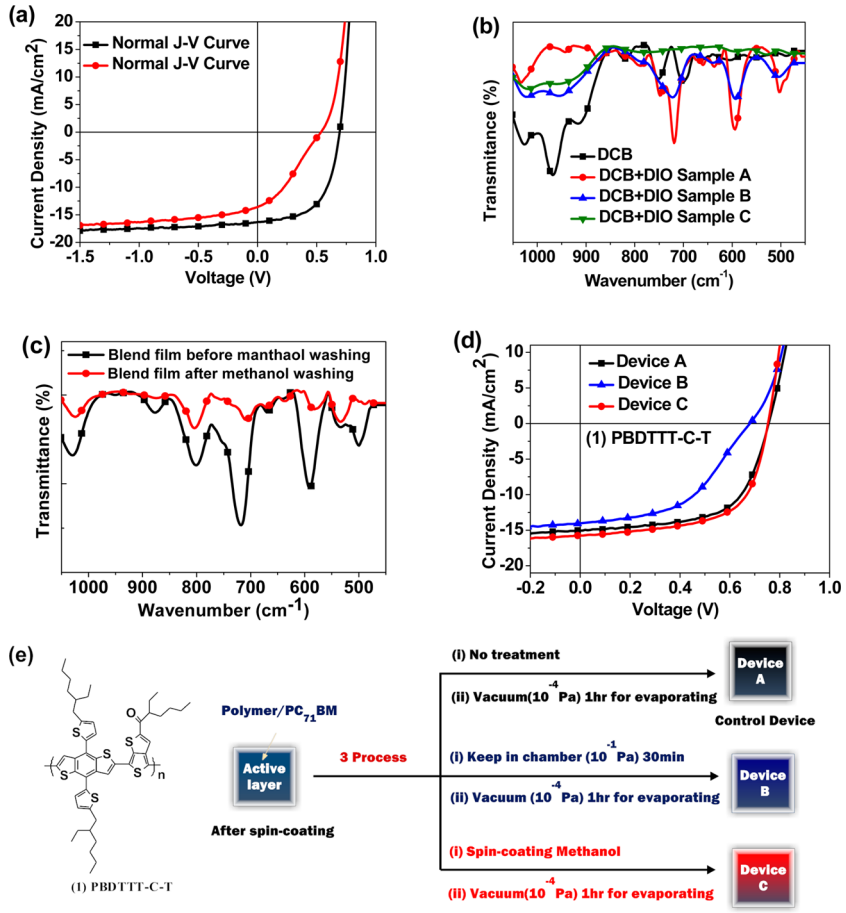

Figure 1. (a) Typical S-shape and normal $J-V$ curves for reference. (b) FT-IR spectra of solvents on KBr plate as prepared at different conditions: Samples A, B, C, and pristine DCB sample for reference. (c) FT-IR spectra of PBDTTT-C-T/$PC_{71}BM$ blend films (spin-coated from the same blend solution with 3% DIO) on KBr plate as prepared at different conditions: before and after methanol treatment. (d) $J-V$ curves with champion PCE results of three kinds of PSC devices based on PBDTTT-C-T/$PC_{71}BM$. (e) Processing procedures of three devices and molecular structure of the model polymer: PBDTTT-C-T.

temperature and pressure. In a previous work, Moulé et al. revealed the role of residual solvent in the P3HT/PCBM system and the effect of residual solvents on the stability of the morphology.[22] Considering that the high vacuum for thermal evaporation process of device fabrication is obtained by two steps: $10^{5}-10^{-1}$ Pa by a mechanical pump and then $10^{-1}-10^{-4}$ Pa by a turbo pump. Under the low vacuum by the mechanical pump, DIO may be evaporated very slowly, but under the high vacuum by the turbo pump, it will be removed from the film quickly. Therefore, the morphology of the active layer would be affected by the slow drying process of the residual DIO, which might be the main reason for the poor reproducibility of the devices. In this work, we investigated the effect of the residual DIO on properties of several high performance polymer/$PC_{71}BM$ photovoltaic systems and designed a series of experiments to identify and then solve the problem caused by the slowing drying process of the residual DIO. Finally, a reasonable interpretation for the phenomenon is also suggested.

RESULTS AND DISCUSSION

First of all, in order to give a solid proof for the presumption of the residual DIO, three samples for FT-IR measurements were prepared by spin-coating a small amount (30 μL) of the mixed solvent of DCB and DIO (v/v, 3/97) onto KBr plates without adding any solute. The first sample was left under glovebox under ambient temperature for 30 min (sample A); the second sample was put into a vacuum chamber (10^{-1} Pa) for 30 min (sample B); the third sample was treated under low vacuum (10^{-4} Pa) for 30 min (sample C). DIO shows characteristic peaks at 720, 595, and 505 cm^{-1}, which are attributed to C−I stretching vibrations.[23] As shown in Figure 1b, the characteristic peaks of DIO can be clearly observed in samples A and B, but the strength of the peaks of sample B is weaker than that of sample A; no peak can be found in sample C. These results clearly indicate that DIO remains on the substrate after spin-coating, while the residual DIO can be evaporated slowly under low vacuum (10^{-1} Pa) and dried completely under high vacuum (10^{-4} Pa). On the basis of these results, it can be concluded that during the spin-coating process DCB dried quickly, but DIO still remained in the blend and then was removed during vacuum preparation process for thermal evaporation. Therefore, it is reasonable to presume that the slow drying process of DIO might affect the morphology of the active layer, and hence if the residual DIO can be removed before the vacuum process, the influence will be avoided. According to a recent work of the Bazan group, post-treatment of the preformed PCX3/PCBM blend film with inert solvent like ethanol offered a simple method for improving the overall device efficiency.[24] Similarly, methanol has a low boiling point

dx.doi.org/10.1021/jp404395q | J. Phys. Chem. C 2013, 117, 14920−14928

and very poor dissolubility (dissolubility <0.01 mg/mL) of the active layer materials but good dissolubility of DIO. Additionally, methanol treatment is a simple modification to PSC devices due to the existence of favorable interfacial dipole by several groups.[25,26] Thus, to wash the active layer with a small amount of methanol might be an effective method to remove the residual DIO and improve the morphological stability. Herein, the blends of PBDTTT-C-T[9,10]/$PC_{71}BM$ were selected as the model system to check the proposed idea.

Figure 1c clearly indicates that when the DCB/DIO mixture was used as processing solvent to make the blend film, the FT-IR spectrum of the blend film showed clear characteristic peaks of DIO, while these peaks disappeared completely by washing with a small amount of methanol. According to the above experiments, it can be concluded the residual DIO can be removed from the blend through three approaches: (1) evaporated under high vacuum quickly; (2) evaporated under low vacuum for a long time; (3) washed out by an inert solvent. As known, morphology of the blends in PSCs is susceptible to the drying process of the solvent. The application of "slow growth",[27] "solvent annealing",[28] or "solvent soaking"[29,30] in P3HT-based PSCs can be seen as the successful examples of morphology control by the drying process of solvents. Therefore, it can be rationally speculated that if the residual DIO is removed by the different methods, morphological properties and hence photovoltaic performance of the PBDTTT-C-T/$PC_{71}BM$ blends will be varied. In order to investigate the influence of the methods of the removal of residual DIO on device performance, three types of devices (Figure 1e) with identical device structure were fabricated and measured in parallel. The active layers of these devices were spin-coated by the same spin speed (900 rpm for 60 s) from the same batch of solution (10 mg/mL for polymer; D/A ratio = 1:1.5; 3% DIO as additive), except that after spin-coating, the blend films were treated by the methods as demonstrated in Figure 1e and thus three types of devices were obtained: Device A: the devices were fabricated by the commonly used approaches; i.e., the devices were put into the chamber for thermal evaporation and the vacuum in the chamber was pumped down as usual (10^5 to 10^{-1} Pa in 5 min and then 10^{-1} to 10^{-4} Pa in 10 min). Device B: the devices were treated with low vacuum (10^{-1} Pa) for 30 min and then pumped down to 10^{-4} Pa for thermal evaporation. Device C: after spin-coating, 50 μL of methanol was dropped onto the blend films and spun off immediately and then the vacuum for thermal evaporation were prepared as for device A. Obviously, in these three types of devices, the residual DIO were removed differently; i.e., for device A, the residual DIO was removed quickly by vacuum; for device B, the residual DIO was evaporated slowly under low vacuum and then completely removed under high vacuum; and for device C, the residual DIO was removed by washing with methanol. Furthermore, to statistically demonstrate the reproducibility of the photovoltaic performance of these three types of devices, 90 pieces of the devices (30 pieces for each condition) were fabricated in parallel by using the same batch of solution of the active layer materials.

The key photovoltaic parameters along with the standard deviations associated with 30 cells are listed in Table 1. The $J-V$ curves with best results of these three kinds of devices are showed in Figure 1d, and the recorded $J-V$ curves are provided in Figure S1. As depicted in Figure 1d, for the best performing devices, the key parameters as well as the shape of the $J-V$ curves of devices A and C are similar, but the PCE of the latter

Table 1. Statistic Photovoltaic Results of PBDTTT-C-T-Based PSCs Associated with 30 Cells Processed at Different Conditions

processing condition	V_{oc} [mV]	J_{sc} [mA/cm^2]	FF [%]	PCE [%]
device A	754 ± 18	14.98 ± 0.49	62.35 ± 1.40	7.07 ± 0.27
device B	650 ± 23	14.18 ± 0.60	46.28 ± 1.91	4.27 ± 0.30
device C	772 ± 5	15.17 ± 0.26	65.03 ± 0.68	7.53 ± 0.12

is slightly higher than that of the former. Interestingly, all devices of the group of device B showed S-curves in $J-V$ measurements. In Figure 1d, the $J-V$ curve of device A showed a series resistance (R_s) of 9.66 Ω cm^2, while that of device C was only 6.57 Ω cm^2 . Interestingly, for device B, an R_s of 39.31 Ω cm^2 can be observed, which is much higher than those of devices A and C, indicating that the blend in device B should have the poorest electric conduction properties (see Figure S2). Statistically, compared to devices A and B, device C showed higher V_{oc} and better FF with low deviation, 772 ± 5 mV and 65.03 ± 0.68%, respectively, and the average J_{sc} of device C was slightly higher than those of devices A and B as well. On the basis of these results, it can be concluded that the PSC devices with methanol treatment (device C) showed better reproducibility; that is, an average PCE of 7.53% of 30 devices was achieved with only ±0.12% variation.

To probe the origin of difference in V_{oc}, peak force−Kelvin probe force microscopy (PF-KPFM)[31] was investigated to provide more information on the surface potential of the organic/metal interface. As shown in Figure 2, the recorded

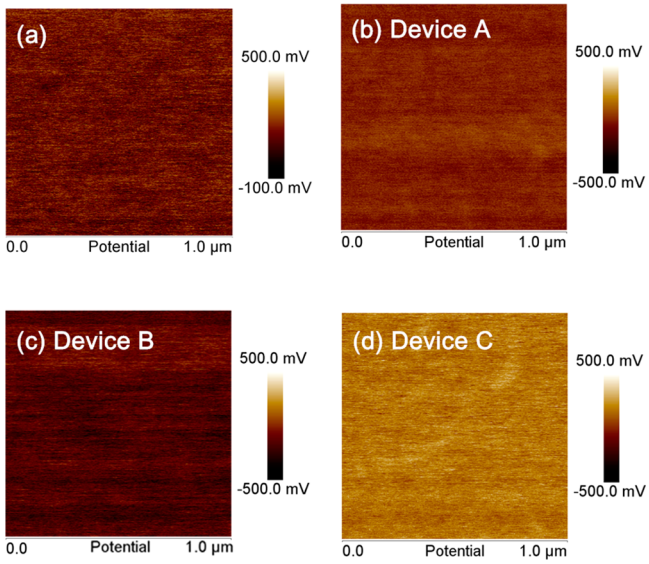

Figure 2. PF-KPFM surface potential images (1 μm × 1 μm) of pure polymer (a) and PBDTTT-C-T/$PC_{71}BM$ blend films in device A (b), device B (c), and device C (d).

work function difference (WFD) of the tip and the top film of active layer of three devices is shown. The WFD_{ave} (the average value deduced from a typical area of 500 nm × 500 nm) of device C was found to rise by ~0.15 V relative to that of device A (see Figure S4), allowing electrons to be collected by the Ca/Al cathode more easily. Thus, methanol treatment lifted the vacuum level on the metal side, thereby reducing the electron injection barrier at the organic/metal interface, and leading to better device performance, which is also verified the findings by

dx.doi.org/10.1021/jp404395q | J. Phys. Chem. C 2013, 117, 14920−14928

other groups in polymer solar cells[24−26] and organic light-emitting diodes.[32] While compared to device C, device B changed oppositely with WFD_{ave} downward ~0.2 V. As the anode is identical for all devices, thus the S-kinks in the $J-V$ curves of device B are attributed to barriers (i.e., causing upward shift of interfacial potential) at the contact between the active layer and the cathode.

Furthermore, water contact angle (WCA) characterizations were used as a tool to gain further insights into the correlation between the process conditions and a semiquantitative method to calculate surface components of the blend films. Thus, the surface composition as well as wettability evolution of the blend films can be well demonstrated.[33]As shown in Figures 3a and 3b, the contact angles of the pure PBDTTT-C-T film and $PC_{71}BM$ film are 104.6° and 81.4°, respectively, implying that if the $PC_{71}BM$ is enriched on the top surface of the blend film, the surface energy will increase and thus the top surface of the film will be more hydrophilic. As shown, the contact angle of the blend film of device A is 100.1°, which is smaller than that of the pure polymer, indicating that the blend film has higher surface energy than the pure polymer film. Interestingly, the blend films of devices B and C are 103.2° and 93.1°, respectively. To quantify the content of $PC_{71}BM$ at the top surface, the fractions of the three blend films were calculated by fitting the contact angle results to the Cassie−Baxter equation.[33] The surface coverage of $PC_{71}BM$ was calculated to decrease from 19.4% in device A to 6.0% in device B and then jump to 49.7% in device C. Therefore, the calculated results clearly suggest that, compared to the blend film of device-A, $PC_{71}BM$ was relatively enriched in the top surface of the blend film of device C but was relatively depleted in that of device B.

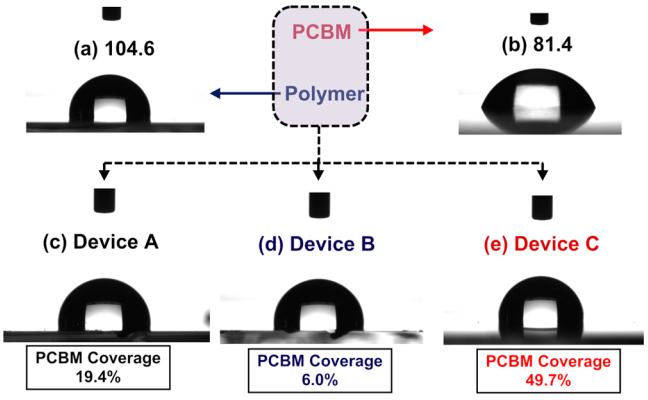

Figure 3. Water contact angle images of the top surface of (a) pure PBDTTT-C-T film, (b) pure $PC_{71}BM$ film, and PBDTTT-C-T/$PC_{71}BM$ (w/w, 1/1.5) blend film in (c) device A, (d) device B, and (e) device C.

In order to verify the above findings and presumption, the compositions of the top surfaces of these three blend films were further characterized by X-ray photoelectron spectroscopy (XPS). As is carefully discussed and reported by Yang et al., XPS is an useful tool to determine the composition of thin surface (0−10 nm) in the P3HT/PCBM photovoltaic system, and the stoichiometric ratio of the components can be calculated directly from the peak intensities of individual elements.[29,35] In the PBDTTT-C-T/$PC_{71}BM$ blend, sulfur can be used as the characteristic element of the polymer because there is no sulfur in $PC_{71}BM$. Therefore, the $PC_{71}BM$ to polymer weight ratios at the top surfaces of the films can be evaluated using C/S atomic ratios obtained from the XPS measurement.[29,35] The compositions of the films spin-coated on glass substrates under different procedures are provided in Table S1. The atomic ratio 8.07 of C 1s and S 2p peaks of the pure polymer is measured, which is close to the C/S stoichiometric ratio of 7.94 in pure polymer. This ensures our test is reliable. Since there is no sulfur in $PC_{71}BM$ molecules, more $PC_{71}BM$ is enriched on the top surface, and higher C/S ratio will be observed. For the blend films of devices A, B, and C, the C/S ratios are 12.81, 12.34, and 13.46, respectively. Thus, the comparison among the XPS and WCA results indicates that when the residual DIO in PBDTTT-C-T/

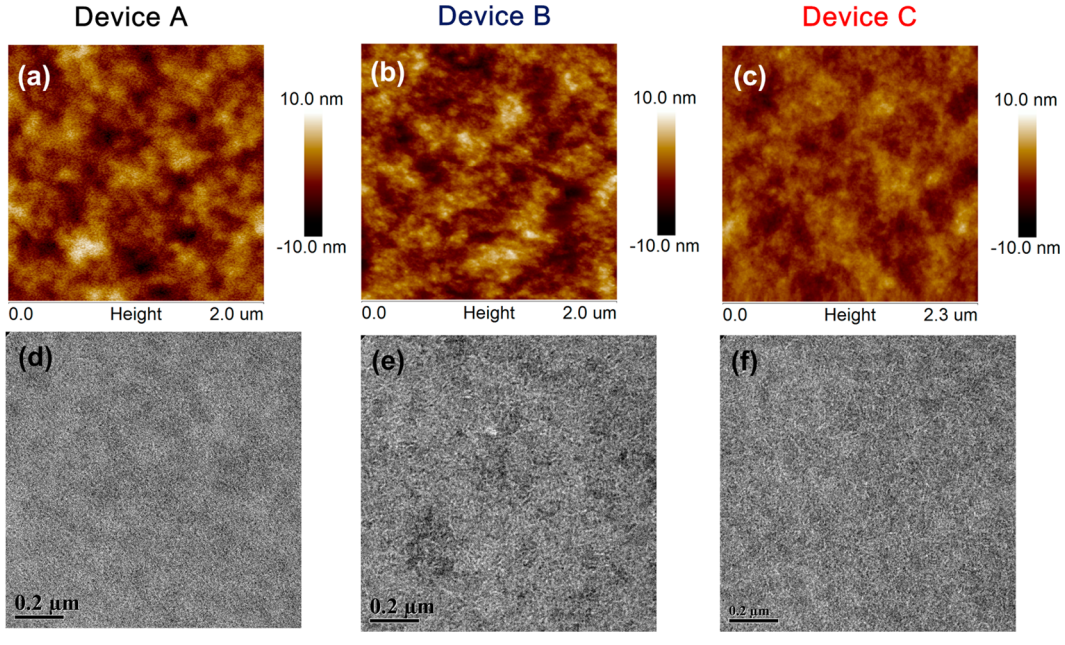

Figure 4. AFM topography (a, b, c) and TEM (c, d, e) images of PBDTTT-C-T/$PC_{71}BM$ blend films in devices A, B, and C, respectively.

dx.doi.org/10.1021/jp404395q | J. Phys. Chem. C 2013, 117, 14920−14928

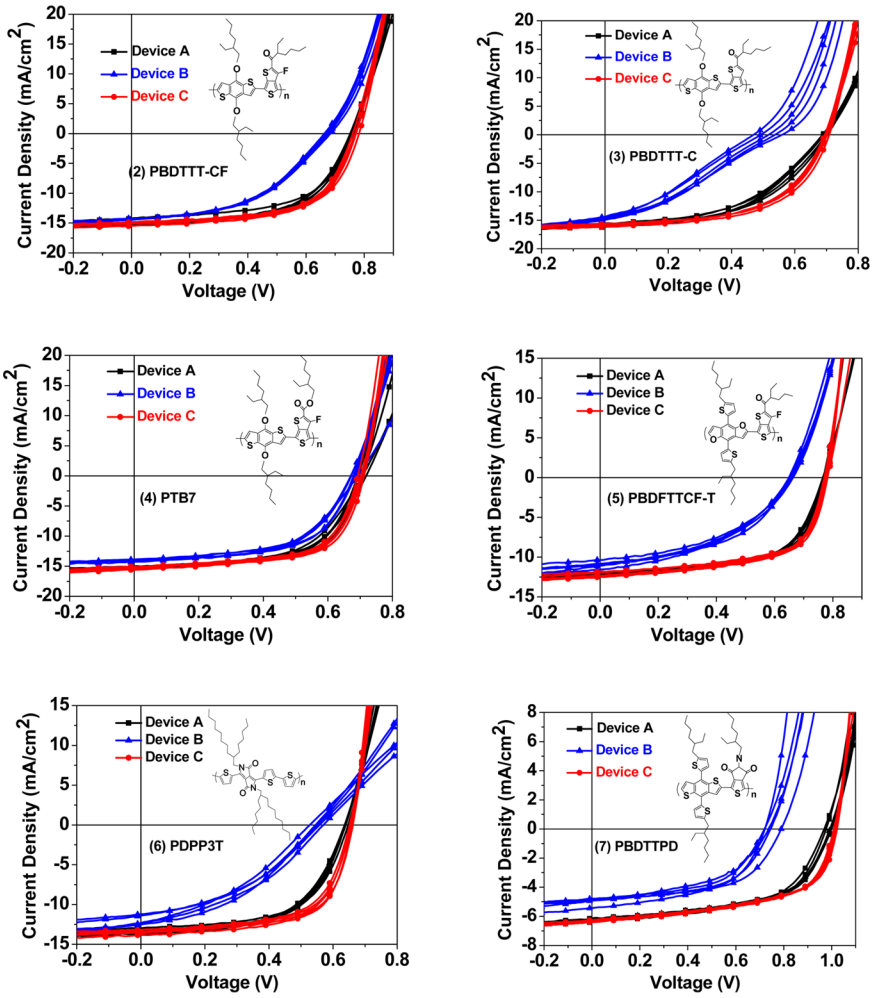

Figure 5. *J*−*V* curves of several representative polymers over five devices for three conditions.

$PC_{71}BM$ film is evaporated slowly under low vacuum, $PC_{71}BM$ will be relatively depleted in the top surface of device B due to the high surface energy,[29] which is contrary to the result by the high-pressure CO_2 treatment;[34] however, when the residual DIO is washed out with methanol, methanol could lock the film and avoid PCBM approaching the bottom surface. Overall, the XPS results are well consistent with the results from WCA measurements and confirmed that $PC_{71}BM$ is relatively enriched in the top surface of the blend film in device C than that of devices A and B.

As the residual additives might lead to difference in morphological features of nanoscale networks, atomic force microscopy (AFM) and transmission electron microscopy (TEM) are employed to measure the surface and bulk morphology. The AFM topography images of devices A−C are shown in Figure 4a−c. From the comparison of topographies, the mean-square surface roughness (R_q) of blend films in devices A, B, and C are 2.20, 2.26, and 1.54 nm, respectively; that is, the blend film in device B exhibits slightly rougher surface while device C is much smoother compared to the film in device A. As depicted in TEM images (Figure 4d−f), the blend film in device B, i.e., after the slow evaporation process of the residual DIO, the film exhibits larger domains with light and dark features, which could be assigned to the aggregations of the polymer and $PC_{71}BM$, respectively.[29] The blend films of device A and especially device C exhibit finer distributed features with smaller domain size, namely more uniform distribution of components.

Then, the results enable us to propose the correlation between reproducibility and the residual DIO in the PSC devices processing with solvent additives. When DIO was used as additive in the o-DCB solution of PBDTTT-C-T/$PC_{71}BM$, DIO cannot be removed from the blend film by the spin-coating process due to the low saturated vapor pressure of DIO under ambient temperature. If the residual DIO is removed slowly under low vacuum, $PC_{71}BM$ will be depleted from the top surface of the blend film due to the high surface energy and hydrophilic nature and also cause severe phase separation of the PBDTTT-C-T/$PC_{71}BM$ blend; if the residual DIO is washed out with methanol, $PC_{71}BM$ will be locked and relatively enriched in the top surface of the blend. The formation of favorable interfacial dipole or contact is broadly used to interpret the correlation between photovoltaic performance and interfacial properties of PSC devices.[16] Therefore, the enriched $PC_{71}BM$ near the cathodic side is favorable for enhancing built-in potential and also reducing the electron collection barrier,[29,36,37] and thus higher PCE as well as better reproducibility can be realized. In both devices A and B, especially for device B, since the residual DIO was slowly removed due to its ultralow saturated vapor pressure, more unfavorable contact was formed due to the extensive depletion of $PC_{71}BM$ in the thin top surface. In device C, since the

dx.doi.org/10.1021/jp404395q | J. Phys. Chem. C 2013, 117, 14920−14928

Table 2. $J-V$ Curves of Several Donors over Five Devices for Three Conditions

donor polymers	processing condition	V_{oc} [mV]	J_{sc} [mA/cm^2]	FF [%]	PCE [%]
PBDTTT-CF (2)	device A2	759 ± 7	15.20 ± 0.97	58.12 ± 1.26	6.79 ± 0.45
	device B2	678 ± 13	14.49 ± 0.24	48.84 ± 1.04	4.81 ± 0.24
	device C2	771 ± 8	15.21 ± 0.18	61.08 ± 1.35	7.12 ± 0.19
PBDTTT-C (3)	device A3	694 ± 7	15.87 ± 0.26	49.20 ± 1.27	5.42 ± 0.22
	device B3	498 ± 28	14.62 ± 0.22	31.09 ± 0.77	2.35 ± 0.23
	device C3	699 ± 6	15.77 ± 0.22	56.32 ± 0.56	6.20 ± 0.12
PTB7 (4)	device A4	702 ± 11	15.34 ± 0.32	60.38 ± 1.43	6.58 ± 0.17
	device B4	679 ± 8	13.95 ± 0.30	57.98 ± 1.45	5.49 ± 0.19
	device C4	707 ± 5	15.46 ± 0.23	63.79 ± 0.72	7.06 ± 0.14
PBDFTTCF-T (5)	device A5	770 ± 4	12.45 ± 0.21	61.83 ± 0.53	5.92 ± 0.18
	device B5	654 ± 6	11.40 ± 0.46	45.10 ± 1.83	3.40 ± 0.24
	device C5	777 ± 3	12.59 ± 0.15	62.27 ± 0.43	6.10 ± 0.10
PDPP3T (6)	device A6	640 ± 4	13.57 ± 0.33	58.20 ± 0.80	5.20 ± 0.18
	device B6	550 ± 15	11.98 ± 0.61	39.65 ± 1.83	2.61 ± 0.21
	device C6	657 ± 4	13.64 ± 0.27	63.59 ± 0.72	5.66 ± 0.15
PBDTTPD (7)	device A7	986 ± 13	6.25 ± 0.12	57.09 ± 0.80	3.52 ± 0.06
	device B7	743 ± 29	4.99 ± 0.26	53.87 ± 3.07	2.00 ± 0.16
	device C7	1014 ± 6	6.45 ± 0.05	57.15 ± 0.32	3.78 ± 0.03

residual DIO was immediately removed by washing with methanol prior to the vacuum process and prevent PCBM from depleting in the top surface, favorable ohmic contact is formed due to the relatively enriched $PC_{71}BM$ in the top surface of the blend film. Therefore, reduced series resistance, lower and stabilized interfacial barrier, and thus higher PCE with better reproducibility will be realized in device C due to the formation of optimal donor/acceptor distribution, smoother surface, and favorable phase separation in the PBDTTT-C-T/$PC_{71}BM$ blend. To concisely characterize the component distribution in the blend film, more advanced techniques like neutron reflectometry or X-ray absorption near-edge reflectometry may be very helpful.[33,38,39]

Furthermore, if the mechanism proposed above is conceptually correct, it should work well in other photovoltaic systems. Therefore, we used different polymers, PBDTTT-CF,[7] PBDTTT-C,[8] PTB7,[15] PBDFTTCF-T,[21] PDPP3T,[40] and PBDTTPD[41] (the molecular structures are inserted in Figure 5), to make these three types of devices (as depicted in Figure 1e) and investigated their photovoltaic performance. According to the reported works, DIO played an important role in improving their photovoltaic performance. On the basis of their photovoltaic parameters (see $J-V$ curves in Figure 5 and Table 2), it is quite clear that the same trend as we observed in the PBDTTT-C-T/$PC_{71}BM$ system was obtained. Interestingly, in all these six photovoltaic systems based on different polymer donors, when the residual DIO was removed slowly as in device B, all these three key parameters (V_{oc}, J_{sc}, and FF) were reduced, and thus PCEs decreased obviously. In the severe cases, the $J-V$ curves of the devices based on PBDTTT-CF, PBDTTT-C, and PDPP3T show S-shaped curves with both obviously low V_{oc}, J_{sc}, and FF (see Table 2), while the $J-V$ curves of the devices based on PTB7, PBDFTT-CF-T, and PBDTTPD exhibit slightly low V_{oc}, J_{sc}, and FF. Very recently, Heeger et al. reported that the efficiency in PTB7/$PC_{71}BM$ is improved system via solvent treatment.[26] The positive effects of solvent treatment are attributed to the improvement of built-in voltage, the decrease in series resistance, and the enhanced charge transport and charge extraction. These results also match well with the above rules.

In short, the positive influence of methanol treatment is a combination of two effects: (i) it provides favorable dipole and forms ohmic contact; (ii) it prevents PCBM from depleting in the top surface by immediately washing out the residual additives. In the device fabrication process, methanol treatment could optimize the cathode's selectivity, namely removal the charge traps as the announcement of Heeger et al. Thus, the bulk recombination could be reduced. On the contrary, the voltage and current loss of the device B can attribute to the poor interface selectivity and the larger phase separation as well as severe recombination in the active layer.

CONCLUSIONS

In conclusion, when a high-T_B solvent was used as additive in PSC device fabrication, the additive remains in the polymer/PCBM blend after spin-coating and residual additive will be evaporated under high vacuum. During the drying process under vacuum, morphology of the blend may be changed, and thus poor reproducibility with lower PCE will be observed in the PSC devices. To wash out the residual high-T_B solvent additives with a little amount of inert solvent prior to the vacuum process for thermal evaporation of metal electrode can be used as a feasible method to improve reproducibility of the PSC devices.

In this work, the blend of PBDTTT-C-T/$PC_{71}BM$ was used as a model system to investigate the correlation between the methods of removal the residual DIO and photovoltaic performance of the PSC devices. By FT-IR characterizations, we confirmed that the residual DIO can be removed by high vacuum and washing with a small amount of methanol. When the residual DIO is evaporated slowly under vacuum, $PC_{71}BM$ will be depleted in the top surface, and thus unfavorable interfacial contact will be formed; when the residual DIO is washed out with methanol, $PC_{71}BM$ will be relatively enriched in the top surface of the blend film, and hence favorable ohmic contact will be formed. After methanol treatment, the device dominated with favorable interfacial contact shows the reduced series resistance and interfacial barrier as well as the smoother and optimal component distribution on the top surface of the active layer, resulting in the higher PCE as well as the better reproducibility.

dx.doi.org/10.1021/jp404395q | J. Phys. Chem. C 2013, 117, 14920−14928

More importantly, the method to solve the problem caused by the residual DIO in the PBDTTT-C-T/$PC_{71}BM$ system can be applied in other polymers, including PBDTTT-CF, PBDTTT-C, PTB7, PDPP3T, and PBDFTTCF-T. Therefore, it should be a simple and universal method in fabrication of high performance PSCs incorporating additives. Furthermore, the results in this work prospectively imply that nonvolatile additives with more complex functionalities may be employed to modulate morphological properties of active layers of PSCs, i.e., to use a nonvolatile additive to control the morphology of a D/A blend and then wash it out with an inert solvent prior to doing thermal evaporation process for metal electrodes.

EXPERIMENTAL SECTION

Materials. PBDTTT-CF,[7] PBDTTT-C,[8] PBDTTT-C-T,[9] PTB7,[15] PBDFTTCF-T,[21] PDPP3T,[40] and PBDTTPD[41] were newly synthesized according to previously reported procedures. The ultradry solvents used in device fabrication process were purchased from Alfa Aesar. The other chemicals are commercial available products and used without any further purification.

Device Fabrication and Characterizations. PSC devices with the typical structure of ITO/PEDOT−PSS (Clevious P VP AI 4083 H. C. Stark, Germany)/PBDTTT-C-T:$PC_{71}BM$ (1:1.5, wt %)/Ca/Al were fabricated under conditions as follows: The ITO-coated glass substrate was cleaned by sequential ultrasonic treatment for 20 min each in detergent, deionized water, acetone, and isopropanol and subsequently dried under a stream of dry nitrogen and then underwent UV-ozone treatment for 20 min. After spin-coating a ∼35 nm layer of PEDOT:PSS onto a precleaned ITO-coated glass substrates, the substrates were dried for 15 min at 150 °C in air and then transferred into a nitrogen glovebox for subsequent procedures. Blend solution were prepared in o-DCB at a concentration of 10 mg/mL (polymer/solvent) and were heated to 50 °C and stirred 5 h for complete dissolution. Then the polymer/$PC_{71}BM$ blend solution was spin-coated after adding 3% (v/v) DIO. For the methanol device, methanol was spin-coated 4000 rpm for 30 s. Process 1: after spin-coating the active layer, the device was left in the glovebox for 30 min and then transferred to the chamber; then the vacuum degree was quickly pumped down to 10^{-4} Pa within 10 min and the same metal electrode (Ca/Al, 20 nm/80 nm) was deposited by thermal evaporation. Process 2: after spin-coating the active layer, the device was transferred to the chamber; the vacuum degree was pumped down to 10^{-1} Pa by mechanical pump and kept at that level for 30 min, and then the turbo pump was turned on to reduce the vacuum degree to 10^{-4} Pa; successively, the metal electrode was deposited by the same condition as used in process 1. Process 3: the same fabrication process was used as that for process 1 except that after the spin-coating, ∼60 μL of methanol was dropped onto the active layer and then spin-coated at 4000 rpm for 30 s. Then the devices were completed by evaporating Ca (20 nm)/Al (80 nm) metal electrodes with area of 0.04 cm^2 defined by masks. The thicknesses of three devices are ca. ∼90 nm as measured by a Bruker DektakXT profilometer. Other photovoltaic polymer-based PSC devices were also fabricated as above procedure under their optimal conditions according to the literatures. The $J-V$ curves were measured under the illumination of 100 mW cm^{-2} AM 1.5G using a XES-70S1 (SAN-EI Electric Co., Ltd.) solar simulator (AAA grade, 70 mm × 70 mm photobeam size). A 2 × 2 cm monocrystalline silicon reference cell (SRC-1000-TC-QZ) was purchased from VLSI Standards Inc. IPCE measurements were performed at Solar Cell Spectral Response Measurement System QE-R3011 (Enli Technoloy Co. Ltd., Taiwan).

X-ray photoelectron spectroscopy data were obtained at the probe length of 10 nm with an ESCALab220i-XL electron spectrometer from VG Scientific using 300 W Al Kα radiation. Samples for PF-KPFM measurements were fabricated in glass substrate coated with ITO on Bruker's Multimode 8 Nanoscope V (Vecco) atomic force microscope. Conductive KPFM probes (backside: 50 nm Al coatings, Bruker) were used throughout the measurements. The WFD images were obtained on a typical area of 0.5 μm × 0.5 μm, over which the average WFD were used. The water contact angle images were performed in the KRÜSS DSA 100 instrument by dropping 3−5 μL of DI water on the pristine films in the air. TEM images were probed by a JEOL 2200FS instrument at 160 kV accelerating voltage. To obtain reliable results, all samples were prepared as the same condition with device fabrication in a N_2 filled-glovebox with O_2 and H_2O content under 0.1 ppm.[38]

ASSOCIATED CONTENT

Supporting Information

Additional $J-V$ data, PF-KPFM, XPS profile, and device characteristics. This material is available free of charge via the Internet at http://pubs.acs.org.

AUTHOR INFORMATION

Corresponding Author

*E-mail: hjhzlz@iccas.ac.cn (J.H.).

Author Contributions

‖Long Ye and Yan Jing contributed equally.

Notes

The authors declare no competing financial interest.

ACKNOWLEDGMENTS

The authors acknowledge the financial support from National High Technology Research and Development Program 863 (2011AA050523), Chinese Academy of Sciences (KJ2D-EW-J01), Ministry of Science and Technology of China, NSFC (Nos. 51173189 and 21104088), and International S&T Cooperation Program of China (2011DFG63460).

REFERENCES

(1) Peet, J.; Kim, J. Y.; Coates, N. E.; Ma, W. L.; Moses, D.; Heeger, A. J.; Bazan, G. C. Efficiency Enhancement in Low-Bandgap Polymer Solar Cells by Processing with Alkane Dithiols. *Nat. Mater.* **2007**, *6*, 497−500.

(2) Lee, J. K.; Ma, W. L.; Brabec, C. J.; Yuen, J.; Moon, J. S.; Kim, J. Y.; Lee, K.; Bazan, G. C.; Heeger, A. J. Processing Additives for Improved Efficiency from Bulk Heterojunction Solar Cells. *J. Am. Chem. Soc.* **2008**, *130*, 3619−3623.

(3) Guo, X.; Cui, C. H.; Zhang, M. J.; Huo, L. J.; Huang, Y.; Hou, J. H.; Li, Y. High Efficiency Polymer Solar Cells Based on Poly(3 hexylthiophene)/Indene-C-70 Bisadduct with Solvent Additive. *Energy Environ. Sci.* **2012**, *5*, 7943−7949.

(4) Hoven, C. V.; Dang, X. D.; Coffin, R. C.; Peet, J.; Nguyen, T. Q.; Bazan, G. C. Improved Performance of Polymer Bulk Heterojunction Solar Cells Through the Reduction of Phase Separation via Solvent Additives. *Adv. Mater.* **2010**, *22*, E63−E66.

(5) Yao, Y.; Hou, J. H.; Xu, Z.; Li, G.; Yang, Y. Effect of Solvent Mixture on the Nanoscale Phase Separation in Polymer Solar Cells. *Adv. Funct. Mater.* **2008**, *18*, 1783−1789.

(6) Moulé, A. J.; Meerholz, K. Controlling Morphology in Polymer−Fullerene Mixtures. *Adv. Mater.* **2008**, *20*, 240−245.

(7) Chen, H. Y.; Hou, J. H.; Zhang, S. Q.; Liang, Y. Y.; Yang, G. W.; Yang, Y.; Yu, L. P.; Wu, Y.; Li, G. Polymer Solar Cells with Enhanced Open-Circuit Voltage and Efficiency. *Nat. Photonics* **2009**, *3*, 649−653.
(8) Hou, J. H.; Chen, H. Y.; Zhang, S. Q.; Chen, R. I.; Yang, Y.; Wu, Y.; Li, G. Synthesis of a Low Band Gap Polymer and Its Application in Highly Efficient Polymer Solar Cells. *J. Am. Chem. Soc.* **2009**, *131*, 15586−15587.
(9) Huo, L. J.; Zhang, S. Q.; Guo, X.; Xu, F.; Li, Y. F.; Hou, J. H. Replacing Alkoxy Groups with Alkylthienyl Groups: A Feasible Approach To Improve the Properties of Photovoltaic Polymers. *Angew. Chem., Int. Ed.* **2011**, *50*, 9697−9702.
(10) Li, X. H.; Choy, W. C. H.; Huo, L. J.; Xie, F. X.; Sha, W. E. I.; Ding, B. F.; Guo, X.; Li, Y. F.; Hou, J. H.; You, J. B.; Yang, Y. Dual Plasmonic Nanostructures for High Performance Inverted Organic Solar Cells. *Adv. Mater.* **2012**, *24*, 3046−3052.
(11) Tan, Z. A.; Zhang, W. Q.; Zhang, Z. G.; Qian, D. P.; Huang, Y.; Hou, J. H.; Li, Y. F. High-Performance Inverted Polymer Solar Cells with Solution-Processed Titanium Chelate as Electron-Collecting Layer on ITO Electrode. *Adv. Mater.* **2012**, *24*, 1476−1481.
(12) Amb, C. M.; Chen, S.; Graham, K. R.; Subbiah, J.; Small, C. E.; So, F.; Reynolds, J. R. Dithienogermole as a Fused Electron Donor in Bulk Heterojunction Solar Cells. *J. Am. Chem. Soc.* **2011**, *133*, 10062−10065.
(13) Chu, T.-Y.; Lu, J.; Beaupre, S.; Zhang, Y.; Pouliot, J.-R.; Wakim, S.; Zhou, J.; Leclerc, M.; Li, Z.; Ding, J.; Tao, Y. Bulk Heterojunction Solar Cells Using Thieno[3,4-c]pyrrole-4,6-dione and Dithieno[3,2-b:2′,3′-d]silole Copolymer with a Power Conversion Efficiency of 7.3%. *J. Am. Chem. Soc.* **2011**, *133*, 4250−4253.
(14) Dou, L. T.; Gao, J.; Richard, E.; You, J. B.; Chen, C. C.; Cha, K. C.; He, Y. J.; Li, G.; Yang, Y. Systematic Investigation of Benzodithiophene- and Diketopyrrolopyrrole-Based Low-Bandgap Polymers Designed for Single Junction and Tandem Polymer Solar Cells. *J. Am. Chem. Soc.* **2012**, *134*, 10071−10079.
(15) Liang, Y. Y.; Xu, Z.; Xia, J. B.; Tsai, S. T.; Wu, Y.; Li, G.; Ray, C.; Yu, L. P. For the Bright Future-Bulk Heterojunction Polymer Solar Cells with Power Conversion Efficiency of 7.4%. *Adv. Mater.* **2010**, *22*, E135−E138.
(16) He, Z. C.; Zhong, C. M.; Huang, X.; Wong, W. Y.; Wu, H. B.; Chen, L. W.; Su, S. J.; Cao, Y. Simultaneous Enhancement of Open-Circuit Voltage, Short-Circuit Current Density, and Fill Factor in Polymer Solar Cells. *Adv. Mater.* **2011**, *23*, 4636−4643.
(17) He, Z. C.; Zhong, C. M.; Su, S. J.; Xu, M.; Wu, H. B.; Cao, Y. Enhanced Power-Conversion Efficiency in Polymer Solar Cells Using an Inverted Device Structure. *Nat. Photonics* **2012**, *6*, 591−595.
(18) (a) Huang, Y.; Guo, X.; Liu, F.; Huo, L. J.; Chen, Y. N.; Russell, T. P.; Han, C. C.; Li, Y. F.; Hou, J. H. Improving the Ordering and Photovoltaic Properties by Extending Pi-Conjugated Area of Electron-Donating Units in Polymers with D-A Structure. *Adv. Mater.* **2012**, *24*, 3383−3389. (b) Qian, D.; Ma, W.; Li, Z.; Guo, X.; Zhang, S.; Ye, L.; Ade, H.; Tan, Z. A.; Hou, J. Molecular Design toward Efficient Polymer Solar Cells with High Polymer Content. *J. Am. Chem. Soc.* **2013**, *135*, 8464−8467.
(19) Ye, L.; Zhang, S. Q.; Ma, W.; Fan, B. H.; Guo, X.; Huang, Y.; Ade, H.; Hou, J. H. From Binary to Ternary Solvent: Morphology Fine-Tuning of D/A Blends in PDPP3T-based Polymer Solar Cells. *Adv. Mater.* **2012**, *24*, 6335−6341.
(20) (a) Qian, D. P.; Ye, L.; Zhang, M. J.; Liang, R. R.; Li, L. J.; Huang, Y.; Guo, X.; Zhang, S. Q.; Tan, Z. A.; Hou, J. H. Design, Application, and Morphology Study of a New Photovoltaic Polymer with Strong Aggregation in Solution State. *Macromolecules* **2012**, *45*, 9611−9617. (b) Zhang, S.; Ye, L.; Wang, Q.; Li, Z.; Guo, X.; Huo, L.; Fan, H.; Hou, J. Enhanced Photovoltaic Performance of Diketopyrrolopyrrole (DPP)-Based Polymers with Extended π Conjugation. *J. Phys. Chem. C* **2013**, *117*, 9550−9557.
(21) Huo, L. J.; Ye, L.; Wu, Y.; Li, Z. J.; Guo, X.; Zhang, M. J.; Zhang, S. Q.; Hou, J. H. Conjugated and Nonconjugated Substitution Effect on Photovoltaic Properties of Benzodifuran-Based Photovoltaic Polymers. *Macromolecules* **2012**, *45*, 6923−6929.
(22) Chang, L. L.; Lademann, H. W. A.; Bonekamp, J. B.; Meerholz, K.; Moulé, A. J. Effect of Trace Solvent on the Morphology of P3HT:PCBM Bulk Heterojunction Solar Cells. *Adv. Funct. Mater.* **2011**, *21*, 1779−1787.
(23) http://riodb01.ibase.aist.go.jp/sdbs/cgi-bin/direct_frame_top.cgi (accessed June 2013).
(24) Liu, X. F.; Wen, W.; Bazan, G. C. Post-Deposition Treatment of an Arylated-Carbazole Conjugated Polymer for Solar Cell Fabrication. *Adv. Mater.* **2012**, *24*, 4505−4510.
(25) (a) Seo, J. H.; Gutacker, A.; Sun, Y. M.; Wu, H. B.; Huang, F.; Cao, Y.; Scherf, U.; Heeger, A. J.; Bazan, G. C. Improved High-Efficiency Organic Solar Cells via Incorporation of a Conjugated Polyelectrolyte Interlayer. *J. Am. Chem. Soc.* **2011**, *133*, 8416−8419. (b) Chen, Y.; Jiang, Z. T.; Gao, M.; Watkins, S. E.; Lu, P.; Wang, H. Q.; Chen, X. W. Efficiency Enhancement for Bulk Heterojunction Photovoltaic Cells via Incorporation of Alcohol Soluble Conjugated Polymer Interlayer. *Appl. Phys. Lett.* **2012**, *100*, 203304.
(26) Zhou, H. Q.; Zhang, Y.; Seifter, J.; Collins, S. D.; Luo, C.; Bazan, G. C.; Nguyen, T.-Q.; Heeger, A. J. High-Efficiency Polymer Solar Cells Enhanced by Solvent Treatment. *Adv. Mater.* **2013**, *25*, 1646−1652.
(27) Li, G.; Shrotriya, V.; Huang, J. S.; Yao, Y.; Moriarty, T.; Emery, K.; Yang, Y. High-Efficiency Solution Processable Polymer Photovoltaic Cells by Self-Organization of Polymer Blends. *Nat. Mater.* **2005**, *4*, 864−868.
(28) Li, G.; Yao, Y.; Yang, H.; Shrotriya, V.; Yang, G.; Yang, Y. "Solvent Annealing" Effect Polymer Solar Cells Based on Poly(3-hexylthiophene) and Methanofullerenes. *Adv. Funct. Mater.* **2007**, *17*, 1636−1644.
(29) Li, H.; Tang, H. W.; Li, L. G.; Xu, W. T.; Zhao, X. L.; Yang, X. N. Solvent-Soaking Treatment Induced Morphology Evolution in P3HT/PCBM Composite Films. *J. Mater. Chem.* **2011**, *21*, 6563−6568.
(30) Li, H.; Chen, Z. B.; Tang, H. W.; Xu, W. T.; Li, J.; Zhao, X. L.; Yang, X. N. An Aqueous Soaking Treatment for Efficient Polymer Solar Cells. *RSC Adv.* **2012**, *2*, 10231−10237.
(31) http://www.brukeraxs.com/fileadmin/user_upload/webinars/slides/High_Resolution_Quantitative_KPFM_PeakForce_webinar_slides_120822.pdf (accessed June 2013).
(32) Wang, Q.; Zhou, Y.; Zheng, H.; Shi, J.; Li, C. Z.; Su, C. M. Q.; Wang, L.; Luo, C.; Hu, D. G.; Pei, J.; Wang, J.; Peng, J. B.; Cao, Y. Modifying Organic/Metal Interface via Solvent Treatment to Improve Electron Injection in Organic Light Emitting Diodes. *Org. Electron.* **2011**, *12*, 1858−1863.
(33) Huang, D. M.; Mauger, S. A.; Friedrich, S.; George, S. J.; Dumitriu-LaGrange, D.; Yoon, S.; Moulé, A. J. The Consequences of Interface Mixing on Organic Photovoltaic Device Characteristics. *Adv. Funct. Mater.* **2011**, *21*, 1657−1665.
(34) Kokubu, R.; Yang, Y. Vertical Phase Separation of Conjugated Polymer and Fullerene Bulk Heterojunction Films Induced by High Pressure Carbon Dioxide Treatment at Ambient Temperature. *Phys. Chem. Chem. Phys.* **2012**, *14*, 8313−8318.
(35) Xu, Z.; Chen, L. M.; Yang, G. W.; Huang, C. H.; Hou, J. H.; Wu, Y.; Li, G.; Hsu, C. S.; Yang, Y. Vertical Phase Separation in Poly(3-hexylthiophene): Fullerene Derivative Blends and Its Advantage for Inverted Structure Solar Cells. *Adv. Funct. Mater.* **2009**, *19*, 1227−1234.
(36) Chen, L. M.; Hong, Z. R.; Li, G.; Yang, Y. Recent Progress in Polymer Solar Cells: Manipulation of Polymer: Fullerene Morphology and the Formation of Efficient Inverted Polymer Solar Cells. *Adv. Mater.* **2009**, *21*, 1434−1449.
(37) Peet, J.; Senatore, M. L.; Heeger, A. J.; Bazan, G. C. The Role of Processing in the Fabrication and Optimization of Plastic Solar Cells. *Adv. Mater.* **2009**, *21*, 1521−1527.
(38) Mauger, S. A.; Chang, L.; Friedrich, S.; Rochester, C. W.; Huang, D. M.; Wang, P.; Moulé, A. J. Self-Assembly of Selective Interfaces in Organic Photovoltaics. *Adv. Funct. Mater.* **2013**, *23*, 1935−1946.

(39) Rochester, C. W.; Mauger, S. A.; Moulé, A. J. Investigating the Morphology of Polymer/Fullerene Layers Coated Using Orthogonal Solvents. *J. Phys. Chem. C* **2012**, *116*, 7287−7292.
(40) Bijleveld, J. C.; Zoombelt, A. P.; Mathijssen, S. G. J.; Wienk, M. M.; Turbiez, M.; de Leeuw, D. M.; Janssen, R. A. J. Poly-(diketopyrrolopyrrole-terthiophene) for Ambipolar Logic and Photovoltaics. *J. Am. Chem. Soc.* **2009**, *131*, 16616−16617.
(41) Piliego, C.; Holcombe, T. W.; Douglas, J. D.; Woo, C. H.; Beaujuge, P. M.; Frechet, J. M. J. Synthetic Control of Structural Order in N-Alkylthieno[3,4-c]pyrrole-4,6-dione-Based Polymers for Efficient Solar Cells. *J. Am. Chem. Soc.* **2010**, *132*, 7595−7596.